RESEARCH ARTICLE | APRIL 19 2023

Sub-femtosecond time-resolved measurements of electron bunches with a C-band radio-frequency deflector in x-ray free-electron lasers 🕩

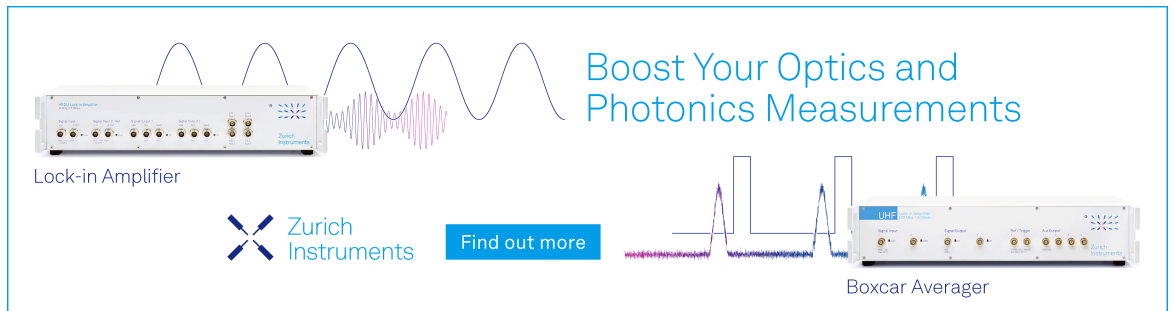Eduard Prat ✉ 🆔 ; Alexander Malyzhenkov 🆔 ; Paolo Craievich ✉ 🆔

Check for updates

CrossMark

View Online

Export Citation

Sub-femtosecond time-resolved measurements of electron bunches with a C-band radio-frequency deflector in x-ray free-electron lasers ⓕ

View Online   Export Citation   CrossMark

Eduard Prat,[a] ⓘ Alexander Malyzhenkov,[b] ⓘ and Paolo Craievich[a] ⓘ

AFFILIATIONS

Paul Scherrer Institut, PSI, CH-5232 Villigen, Switzerland

[a] Authors to whom correspondence should be addressed: eduard.prat@psi.ch and paolo.craievich@psi.ch
[b] Present address: CERN, CH-1211 Geneva 23, Switzerland.

ABSTRACT

Time-resolved diagnostics are fundamental for x-ray free-electron lasers (FELs). Radio-frequency (RF) transverse deflector structures (TDSs) are typically employed to characterize the temporal properties of the electron beams driving FELs. In this article, we present time-resolved measurements with a resolution below one femtosecond using a C-band RF TDS at SwissFEL, the x-ray FEL facility at the Paul Scherrer Institute in Switzerland. The sub-femtosecond resolution is partially achieved due to an optimized optics setup and fits the expected values, showing a good understanding of our models. Measurements with a sub-femtosecond resolution are of crucial importance for ultra-fast x-ray FEL applications.

Measuring the temporal properties of electron beams is of fundamental importance in electron accelerators. In this article, we focus on x-ray free-electron lasers (FELs),[1–3] which are revolutionary tools to observe matter with time and spatial resolution at the atomic level. X-ray FEL radiation is generated by a multi-GeV high-brightness electron beam traveling through an undulator beamline. Standard x-ray FEL pulses have peak powers at the gigawatt level and durations of a few tens of femtoseconds or shorter. Ultra-short FEL pulses at the femtosecond level and below, achieved with ultra-short electron beams or with spoiling methods,[4–7] are required to study ultra-fast atomic and molecular processes.[8]

The FEL performance is determined by the electron bunch duration and the time-resolved properties of the electron beam, such as the current profile and the slice emittance, so it is of crucial importance to measure and optimize such properties. The longitudinal phase space (energy vs time coordinates) of the electron beam is of particular interest. In addition to providing information on the electron beam energy chirp, the measurement, if done after the

undulator, allows for the reconstruction of the FEL power profile by comparing lasing-disabling and lasing-enabling conditions.[9,10]

Radio-frequency (RF) transverse deflection structures (TDSs) are well known diagnostics devices for the characterization of the temporal properties of electron bunches in linear accelerators.[11–21] A TDS-based diagnostic system streaks (or, using the terminology for this type of device, shears or stretches) a charged bunch in the transverse direction by introducing a correlation between the transverse momentum and the longitudinal position in the bunch. This correlation can be used to image on a screen the longitudinal distribution of the particles if a suitable beam optics setup is used. One of the main advantages of the TDS-based systems is that the image on the screen represents a single-shot measure of the time profile of the bunch.

To our knowledge, only one working group has achieved sub-femtosecond resolution using, in that case, an X-band (with a frequency f of 11.4 GHz) RF TDS system and in the soft x-ray regime.[10] In this article, we present sub-femtosecond measurements

13 March 2024 10:35:40

with a C-band (f = 5.7 GHz) RF TDS system for charged bunches with 5.2 GeV energy used to generate FEL in the hard x-ray regime (x rays with photon energies of about 5 keV or higher). As the streaking scales linearly with the RF frequency, reaching sub-femtosecond resolution is more challenging with a C-band TDS. In comparison with X-band TDSs, C-band systems have the advantages of being more affordable and accessible. Moreover, they have larger apertures, thus allowing operation with larger electron beam sizes and being less affected by wakefields. The measurements were performed at SwissFEL,[22] the x-ray FEL facility at the Paul Scherrer Institute in Switzerland.

The absolute calibration factor C between the transverse coordinate on a screen and the time coordinates within the electron bunch is obtained by measuring the dependence of the transverse position of the centroid of the streaked beam on the RF phase of the TDS. This calibration is sometimes called the streaking factor. Once the calibration is known, the electron pulse duration is simply obtained as the streaked beam size divided by the calibration. A more sophisticated and precise measurement can be obtained by measuring the streaked beam sizes for the two zero-crossings of the deflector.[14,23] Such a measurement can overcome an initially streaked electron beam (in such a case, measuring only one zero-crossing would over- or underestimate the electron beam pulse duration).

The measurement resolution R is normally defined as the unstreaked beam size σ_0 divided by the calibration factor C: $R = \sigma_0/C$.[12] For relativistic electrons and assuming that the deflector is operating around the zero-crossing point, the resolution can be obtained from the electron beam and deflector parameters as follows:

TABLE I. Main RF parameters for the C-band TDSs. The operational temperature is 30 °C for both TDSs. The definition of the shunt impedance is $R_s = -E_T^2/(2dP/dz)$, where E_T is the equivalent deflecting voltage and P is the RF power.

Parameters		Unit
Frequency	5712	MHz
Dipole mode	$5\pi/6$	
Total length	1830	mm
Effective length	1723.651	mm

	Measurements			
	TDS1	TDS2	Target	
Phase error	±4.1	±4.0	<±5	deg
Shunt impedance	21.2	21.2	≥20	MΩ/m
Attenuation	0.531	0.530	0.54 ± 0.02	Np
Filling time	258	259	270	ns
Unloaded Q	8731	8785	≤7500	
Group velocity	0.0223c	0.0222c	0.021c	
Power-to-voltage	6.83	6.83	≥6.67	MV/MW$^{0.5}$

2x TDSs + BOC		
BOC Q_0	216 000	
BOC β	10	
RF pulse length	3	μs
Power-to-voltage	15.42	MV/MW$^{0.5}$

$$R = \frac{\sqrt{\frac{\varepsilon}{\gamma}}E}{\sqrt{\beta}\sin(\mu)eVck}, \qquad (1)$$

where ε is the normalized emittance of the electron beam in the streaking plane, γ is the Lorentz factor of the electron beam, E is the electron beam energy, β is the β-function in the streaking plane at the deflector location, $\sin\mu$ is the phase advance in the streaking direction between the deflector and the profile monitor, e is the elementary charge, V is the deflector voltage, c is the speed of light, and $k = 2\pi f/c$ is the wavenumber of the deflector (for our case, k = 119.7 m^{-1}). As usual, $E = \gamma m_e c^2$, with $m_e c^2 \approx 0.511$ MeV the rest energy of an electron.

The SwissFEL LINAC consists of three C-band sections, comprising a total of 26 RF modules, each with four two-m long acceleration structures. Each module has a single 50 MW C-band klystron, which amplifies an RF pulse of up to 3 μs duration. Furthermore, each module includes a barrel-open cavity (BOC) pulse compressor to increase peak power by up to a factor of 6.[24] The last C-band module of the LINAC shares, through a vacuum RF switch, the power source with the two TDSs. The RF repetition rate is 100 Hz, the same as the maximum machine frequency, allowing shot-to-shot measurements at the full repetition rate. Nevertheless, the bunch rate is normally reduced to 1 Hz when the TDSs are used to reduce radiation losses. Installing additional radiation shielding in the accelerator tunnel would mitigate operational issues related to beam loss. The RF pulse compressed by the BOC is evenly distributed between the two C-band TDSs through the use of a 3 dB power splitter. In this way, each TDS can be driven with approximately the same peak RF power minus the RF losses arising from the waveguide network. An estimate of the total attenuation of the RF power distribution system, which includes waveguide attenuation and insertion losses, resulted in a value of −0.86 dB corresponding to a power

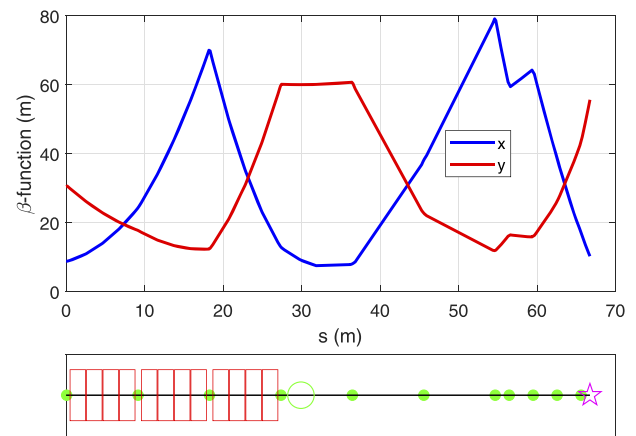**FIG. 1.** Measurement optics and setup. Top: β-function along the lattice. Bottom: sketch of the measurement setup, where s corresponds to the longitudinal direction along the accelerator, the red boxes correspond to the RF accelerating structures, the big green circle indicates the C-band TDSs, the small green circles correspond to the quadrupole magnets, and the magenta star indicates the profile monitor.

loss of 18%. The C-band TDS is of the RAIDEN structure developed for the SACLA FEL project and manufactured by Mitsubishi Heavy Industries, Ltd. (MHI).[19] It is a cylindrical waveguide periodically loaded with uniform irises shaped in the form of racetracks. The iris consists of two semicircles with radii of 6 mm and two straight lines of length 8 mm, connected alternately. The racetrack-shaped irises break the axial symmetry and provide the separation of the two polarizations of the dipole mode. Table I lists the main RF parameters for the two C-band TDSs. The two structures have a constant impedance and work with a backward-traveling wave with a vertical dipole HEM11-5π/6 mode. The power-to-voltage coefficient is also estimated for the system comprising two TDSs and the BOC, taking into account the attenuation in the waveguide system.

Figure 1 shows the measurement optics and a sketch of the setup. The C-band TDSs are located at the end of the SwissFEL LINAC, before the energy collimator and the hard x-ray undulators. Since our TDSs are installed before the undulator beamline,

reconstructing the FEL power profile as done in Ref. 10 is not feasible with our current setup—this would be possible by placing the TDS system after the undulators. As an alternative for such measurements, we presently use the wakefields of a corrugated structure installed after the hard x-ray undulator beamline.[25] The transverse distribution of the electrons is measured with a Ce:YAG scintillator screen[26] located 37 m downstream of the TDSs. The measurement optics were designed to have an optimum deflector resolution [see Eq. (1)] while keeping the quadrupole magnet fields within reasonable limits. First, the β-function at the deflector is set to the relatively large value of 60 m. Second, the phase advance between the deflector and the profile monitor is set to 88° so that $\sin \mu \approx 1$. Last, the β-function at the profile monitor location is set to the relatively large value of 56 m so that the unstreaked beam size can be measured with a good resolution.

The measurements were done for a bunch charge of 10 pC, suitable for short-pulse operation,[6] and an electron beam energy of 5.2 GeV. The beam optics were empirically matched at the injector

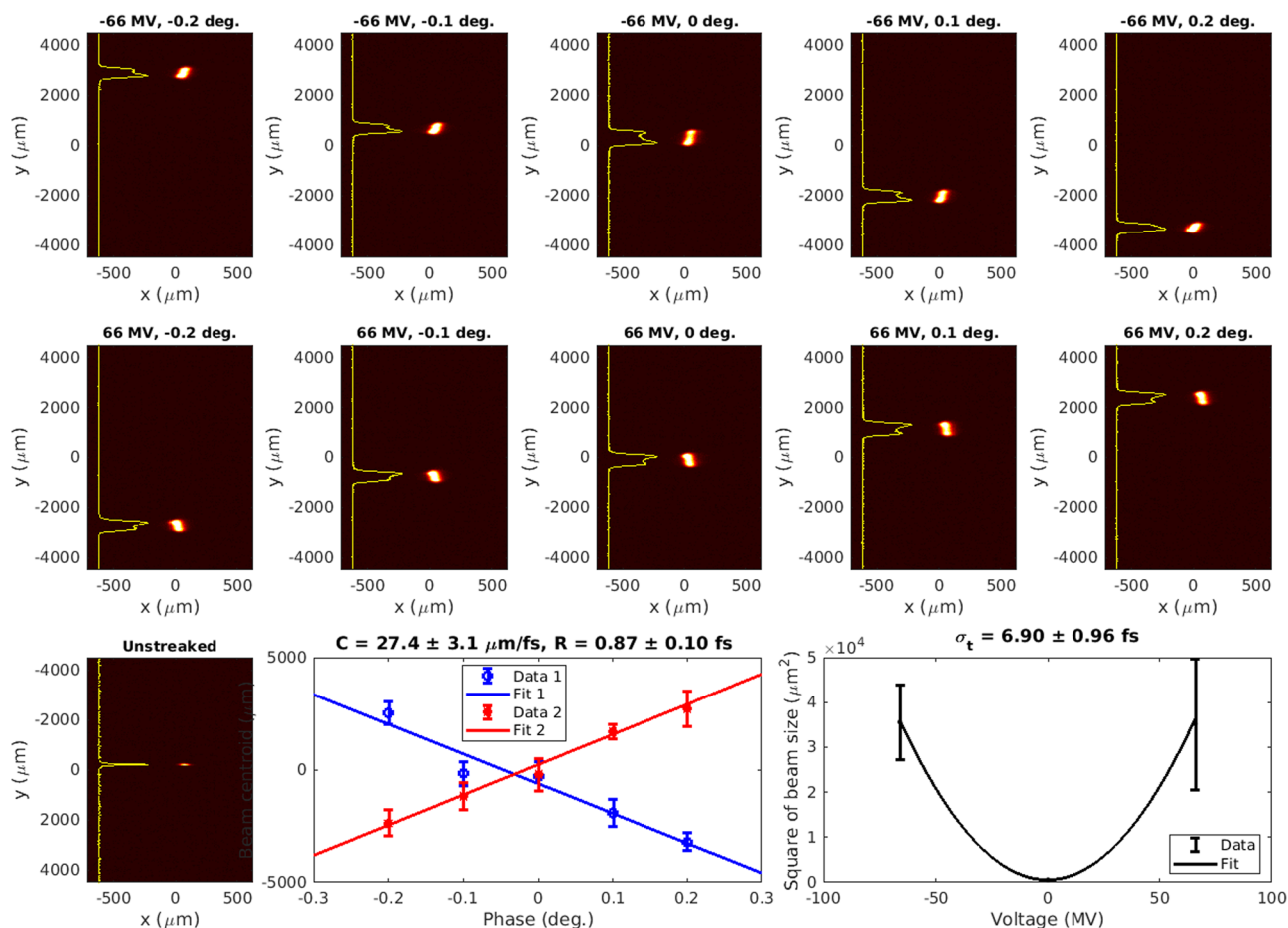**FIG. 2.** Measurement. Top/center: single-shot streaked images for different phases at the first/second zero-crossing. Bottom left: single-shot unstreaked image. Bottom center: measured and fitted beam centroid variation as a function of the beam phase for the two zero-crossings. Bottom right: measured and fitted beam size squared for streaked and unstreaked cases. See the text for more details.

and set to design values afterward. Therefore, we expect a vertical β-function of 60 m at the deflector position, a β-function of 56 m at the profile monitor location, and a phase advance between the two locations fulfilling $\sin \mu \approx 1$. Using the symmetric single-quadrupole scan technique,[27] we measured the projected emittance after the first bunch compressor to be 68 nm in the horizontal plane and 76 nm in the vertical direction. We then set the deflector voltage to the maximum possible to limit RF breakdowns, estimated to be 66 MV. The streaked beam size was measured for five different phases at each of the two zero-crossings. We took five shots at each measurement point. The error bars shown later for different measured parameters correspond to the statistical uncertainty of the reconstructed values.

Figure 2 shows the measurement results. The upper and center plots display single-shot images of the streaked beam for the different phases at the two zero-crossings. The bottom-left plot shows a single-shot image for the unstreaked beam size, which has a value of 23.8 ± 0.3 μm. The expected natural beam size is $\sigma_0 = \sqrt{\beta_p \varepsilon / \gamma}$, where β_p is the β-function at the profile monitor location and $\gamma \approx (5.2 \text{ GeV}/0.511 \text{ MeV})$. From our optics design ($\beta_p = 56$ m) and the measured emittance of 76 nm, we expect a beam size of 20.5 μm, in reasonable agreement with our measurement of 23.8 μm. The difference may be attributed to the profile measurement resolution.

In the bottom-center plot, we display how the centroid of the streaked beam changes with the deflector phase for the two zero-crossings. A linear fit to the data at each zero-crossing gives a calibration factor of -27.1 ± 5.5 μm/fs for the first zero-crossing and 27.6 ± 2.8 μm/fs for the second zero-crossing. The average calibration factor comes out to be $C = 27.4 \pm 3.1$ μm/fs. The error bars shown in the right center plot are 571 μm (averaged over the ten measured phases). This corresponds to 20.8 fs or 0.04 degrees of the C-band TDS and includes the beam arrival time and RF jitter. Our measurement uncertainties could be reduced by measuring the TDS phase jitter on a single-shot basis. However, we do not expect a very significant improvement considering that the RF jitter (maximum $0.04°$) is at least ten times smaller than the phase variation in the measurement ($0.4°$).

Dividing the measured natural beam size with the calibration, we obtain a resolution of $R = 0.87 \pm 0.10$ fs. The expected resolution obtained with Eq. (1) and our electron beam and deflector parameters ($\varepsilon = 76$ nm, $E = 5.2$ GeV, $\beta = 60$ m, $V = 66$ MV, and $k = 119.7$ m^{-1}) is 0.77 fs. The discrepancy between the measured and expected resolutions can be due to, as mentioned earlier, the profile monitor resolution, a not perfectly matched beam, or an underestimation of the attenuation in the waveguide network.

Following Refs. 14 and 23, we fit a parabola to the square of the streaked and unstreaked beam sizes to obtain the bunch duration. The bottom-right plot of Fig. 2 shows the measured and fitted squares of the unstreaked and streaked beam sizes for each zero-crossing at zero phase. The resulting bunch duration is 6.90 ± 0.96 fs (the rms value).

To conclude, we have demonstrated sub-femtosecond resolution in time-resolved electron beam measurements using a C-band RF system at SwissFEL. Such measurements will play an important role in many x-ray FEL applications studying ultra-fast phenomena. Our sub-femtosecond temporal resolution is achieved as a result of an optimized optics setup. In particular, a relatively large β-function at the TDS and a suitable phase advance between the TDS and the profile monitor directly improve the resolution, and a large enough β-function at the profile monitor limits the negative impact of the transverse resolution of the profile monitor. The reasonable agreement between the measured and expected resolution shows a good understanding of our optics model and our overall RF system, which is indispensable to achieve the expected performance of TDSs.

AUTHOR DECLARATIONS

Conflict of Interest

The authors have no conflicts to disclose.

Author Contributions

Eduard Prat: Conceptualization (equal); Data curation (equal); Formal analysis (equal); Investigation (equal); Methodology (equal); Software (lead); Supervision (equal); Validation (equal); Visualization (lead); Writing – original draft (equal); Writing – review & editing (equal). **Alexander Malyzhenkov**: Conceptualization (equal); Data curation (equal); Formal analysis (equal); Investigation (equal); Methodology (equal); Validation (equal); Writing – review & editing (equal). **Paolo Craievich**: Conceptualization (equal); Data curation (equal); Formal analysis (equal); Investigation (equal); Methodology (equal); Resources (lead); Supervision (equal); Validation (equal); Writing – original draft (equal); Writing – review & editing (equal).

DATA AVAILABILITY

The data that support the findings of this study are available from the corresponding authors upon reasonable request.

REFERENCES

[1] B. W. J. McNeil and N. R. Thompson, Nat. Photonics **4**, 814 (2010).

[2] C. Pellegrini, A. Marinelli, and S. Reiche, Rev. Mod. Phys. **88**, 015006 (2016).

[3] C. Bostedt, S. Boutet, D. M. Fritz, Z. Huang, H. J. Lee, H. T. Lemke et al., Rev. Mod. Phys. **88**, 015007 (2016).

[4] S. Huang, Y. Ding, Y. Feng, E. Hemsing, Z. Huang, J. Krzywinski et al., Phys. Rev. Lett. **119**, 154801 (2017).

[5] A. Marinelli, J. MacArthur, P. Emma, M. Guetg, C. Field, D. Kharakh, A. A. Lutman, Y. Ding, and Z. Huang, Appl. Phys. Lett. **111**, 151101 (2017).

[6] A. Malyzhenkov, Y. P. Arbelo, P. Craievich, P. Dijkstal, E. Ferrari, S. Reiche, T. Schietinger, P. Juranić, and E. Prat, Phys. Rev. Res. **2**, 042018(R) (2020).

[7] J. P. Duris, J. P. MacArthur, J. M. Glownia, S. Li, S. Vetter, A. Miahnahri et al., Phys. Rev. Lett. **126**, 104802 (2021).

[8] L. Young, K. Ueda, M. Gühr, P. H. Bucksbaum, M. Simon, S. Mukamel et al., J. Phys. B: At., Mol. Opt. Phys. **51**, 032003 (2018).

[9] Y. Ding, C. Behrens, P. Emma, J. Frisch, Z. Huang, H. Loos, P. Krejcik, and M.-H. Wang, Phys. Rev. ST Accel. Beams **14**, 120701 (2011).

[10] C. Behrens, F.-J. Decker, Y. Ding, V. A. Dolgashev, J. Frisch, Z. Huang, P. Krejcik, H. Loos, A. Lutman, T. J. Maxwell, J. Turner, J. Wang, M.-H. Wang, J. Welch, and J. Wu Nat. Commun. **5**, 3762 (2014).

13 March 2024 10:35:40

[11] I. Ben-Zvi, J. X. Qui, and X. J. Wang, in *Proceedings of the 1997 Particle Accelerator Conference, Vancouver, Canada* (IEEE, Piscataway, 1998), pp. 1971–1975.

[12] R. Akre, L. Bentson, P. Emma, and P. Krejcik, in *Proceedings of the 2001 Particle Accelerator Conference, Chicago* (IEEE, Piscataway, 2001), pp. 2353–2355.

[13] D. Alesini, G. Di Pirro, L. Ficcadenti, A. Mostacci, L. Palumbo, J. Rosenzweig, and C. Vaccarezza, Nucl. Instrum. Methods Phys. Res., Sect. A **568**, 488 (2006).

[14] D. Alesini, Int. J. Mod. Phys. A **22**, 3693 (2007).

[15] S. Korepanov, M. Krasilnikov, F. Stephan, D. Alesini, and L. Ficcadenti, in *Proceedings of DIPAC 2007, Venice, Italy* (Elettra, Trieste, 2008), pp. 144–146.

[16] M. Röhrs, C. Gerth, H. Schlarb, B. Schmidt, and P. Schmüser, Phys. Rev. ST Accel. Beams **12**, 050704 (2009).

[17] V. A. Dolgashev, G. Bowden, Y. Ding, P. Emma, P. Krejcik, J. Lewandowski, C. Limborg, M. Litos, J. Wang, and D. Xiang, Phys. Rev. Accel. Beams **17**, 102801 (2014).

[18] P. Craievich, M. Petronio, S. G. Biedron, D. Castronovo, M. D. Forno, S. D. Mitri, N. Faure, D. L. Civita, G. Penco, L. Rumiz, L. Sturari, R. Vescovo, and D. Wang, IEEE Trans. Nucl. Sci. **62**, 210 (2015).

[19] H. Ego, H. Maesaka, T. Sakurai, Y. Otake, T. Hashirano, and S. Miura, Nucl. Instrum. Methods Phys. Res., Sect. A **795**, 381 (2015).

[20] P. Craievich, M. Bopp, H.-H. Braun, A. Citterio, R. Fortunati, R. Ganter *et al.*, Phys. Rev. Accel. Beams **23**, 112001 (2020).

[21] J. Tan, W. Fang, D. Tong, Q. Gu, X. Huang, Z. Li, T. Higo, S. Matsumoto, T. Takatomi, and Z. Zhao, Nucl. Instrum. Methods Phys. Res., Sect. A **930**, 210 (2019).

[22] E. Prat, R. Abela, M. Aiba, A. Alarcon, J. Alex, Y. Arbelo *et al.*, Nat. Photonics **14**, 748 (2020).

[23] R. Akre, L. Bentson, P. Emma, and P. Krejcik, in *Proceedings of EPAC2002, Paris, France* (EPS-IGA and CERN, Geneva, 2002), pp. 1882–1884.

[24] R. Zennaro, M. Bopp, A. Citterio, R. Reiser, and T. Stapf, in *Proceedings of IPAC 2013, Shanghai, China* (JACoW, Geneva, 2013), pp. 2827–2829, WEPFI059.

[25] P. Dijkstal, A. Malyzhenkov, P. Craievich, E. Ferrari, R. Ganter, S. Reiche, T. Schietinger, P. Juranić, and E. Prat, Phys. Rev. Res. **4**, 013017 (2022).

[26] R. Ischebeck, E. Prat, V. Thominet, and C. Ozkan Loch, Phys. Rev. ST Accel. Beams **18**, 082802 (2015).

[27] E. Prat, Nucl. Instrum. Methods Phys. Res., Sect. A **743**, 103 (2014).

13 March 2024 10:35:40